Direct Observation of the Intermittency of Intense Vorticity Filaments in Turbulence

S. Douady, Y. Couder, and M. E. Brachet
Laboratoire de Physique Statistique, 24 rue Lhomond, 75231 Paris CEDEX 05, France
(Received 25 February 1991)

Cavitation in a liquid seeded with bubbles is used as a new visualization technique to single out the regions of very low pressure of a fully developed turbulent flow. By this means, the sudden appearance of high vorticity filaments is observed. These structures are very thin and short lived and display a high degree of temporal as well as spatial intermittency. They contribute to the flow organization: In particular their disintegration corresponds to the formation of large eddies.

PACS numbers: 47.25.−c, 47.55.Bx, 47.80.+v

Measurements and visualization are both difficult in the investigation of 3D fully developed turbulence. The extent of the flow and its rapid evolution means that an overwhelming quantity of information should be recorded and treated to obtain the spatial structure of the flow as well as its temporal evolution. But the experimentalists can only, for instance, measure the velocity at a single point of a turbulent flow. The analysis of time series of measurements of this type [1] has permitted deduction of the energy spectrum of a steady regime of turbulence and thus a verification of the phenomenological theory of Kolmogorov [2]. However, in this type of approach most of the flow's spatial structure and dynamics are lost. Reconsidering recently such velocity time series, it was shown that they exhibit intermittent bursts of velocity (see, for instance, Refs. [3] and [4]). These are usually ascribed to the advection, near the point of measurement, of strong vortices (often called coherent structures) but give very little information about them.

Theoretically, two fields are studied in order to characterize the inhomogeneity of turbulence: the vorticity $\omega=\nabla\times\mathbf{v}$ [or $\omega^2=\frac{1}{2}\sum_{ij}(\partial_i v_j-\partial_j v_i)^2$] and the energy dissipation $\rho\nu\sigma^2$ [where $\sigma^2=\frac{1}{2}\sum_{ij}(\partial_i v_j+\partial_j v_i)^2$], $\mathbf{v}$ being the local fluid velocity, ρ the density, and ν the kinematic viscosity. It has been known for some time, through numerical simulations, that the high-level vorticity is concentrated in filaments [5–7]. More recently, simulations [8–10] of the Taylor-Green vortex [11], while confirming a repartition of the vorticity in tubes, showed that the energy dissipation is distributed on sheets [9,10].

In experiments, the visualization techniques have mainly been concerned with the transient advection of passive scalars and it has not been possible yet to visualize directly the vorticity field. As for the strain field, only the recent observation of the orientation of thin platelets in a turbulent flow has permitted one to infer a layered structure [12], apparently in agreement with the dissipation sheets of the simulations.

In the present work we seek to observe experimentally the dynamics and the topology of the high vorticity regions. *The basic idea is that it is possible to single them out and visualize them because they correspond to the regions of low pressure where a cavitation effect can take place.* This possibility is linked with the equation relating the pressure field p with the vorticity and the dissipation, a relation which has not hitherto been given much attention. By taking the divergence of the Navier-Stokes equations, in a constant-density incompressible fluid, we find

$$2\Delta p/\rho+\sigma^2-\omega^2=0\,.$$

It is natural to establish an *analogy to electrostatics, with the pressure corresponding to the potential resulting from negative and positive charges distributed in proportion to the square of vorticity and the energy dissipation, respectively.* The vorticity concentrations thus act as sources of low pressure and their greatest relative concentration will cause strong depressions.

The conditions for proper cavitation are controlled by the ratio of the dynamic pressure with the difference between the atmospheric pressure and the vapor pressure of the fluid. With water in ordinary conditions of pressure and temperature, cavitation is only observed in very strongly stirred liquids, usually near a moving boundary (e.g., at the tips of a submarine's propeller). However, the threshold can be lowered in two cases: If the fluid contains a diluted gas or if it contains already formed microbubbles. We tried both techniques and found the latter to be simpler. No nucleation process is involved; before starting the experiment the fluid is seeded with a large number of very small bubbles and the "cavitation" results from the migration of some bubbles to the low-pressure regions.

We wished to investigate a steady bulk turbulent flow, in which the energy is constantly injected at a large scale and which could be compared with numerical simulations. We therefore built the cell sketched in Fig. 1. It is comprised of a vertical cylindrical container of diameter 15 cm and height 23 cm. The cell is filled with water with a free surface near the top. Immersed at each end of the cylinder is a rotating disk of radius R_0 (5 cm) with protruding rims (2 cm high). These two disks, 156 cm apart from each other, can be rotated independently at angular velocities ranging from 0 to 15 Hz. We rotate them at exactly the same velocity Ω_0 in opposite directions. The fluid at the top and bottom of the cell is thus forced into two opposite rotations separated by a strong shear in the median plane of the cell. Two secondary

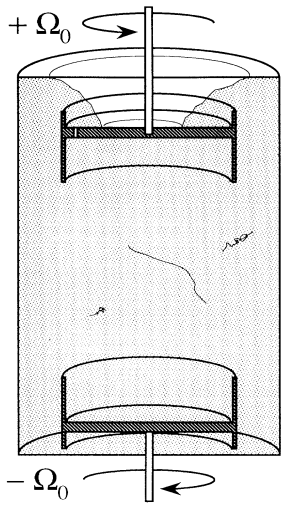

FIG. 1. Cross section of the experimental cell (see text).

toroidal recirculations are also present [13]. The main turbulence is generated in the median region of the cell and is due to the shear, stretched by the recirculations. The diameter of the largest eddies observed in the shear is of the order of the disk's radius R_0, showing this scale to be the energy injection scale L_I. The characteristic velocity U_I in these eddies is of the order of the mean disk rotation velocity $\Omega_0 R_0/2$. Therefore we estimate the corresponding integral Reynolds number to be of the order of $R_I = U_I L_I/\nu \approx \Omega_0 R_0^2/2\nu$. Thus in this small tank filled with water we mainly worked at Reynolds numbers of the order of 80000 for $\Omega_0/2\pi = 10$ Hz. Note that this flow is somewhat similar in geometry to the Taylor-Green vortex [11]. The latter, however, is periodic with free-slip boundaries, while our experimental flow is contained by the tank and the disks. In order to estimate the power injected in the turbulent flow we measure at each rotation frequency the difference between the electrical power needed to rotate the disks with and without the fluid. We find $W = 0.02(\Omega_0/2\pi)^3$, where W is expressed in watts. This power law is consistent with Kolmogorov's scaling and the prefactor is in agreement with previous numerical results [14].

In our cavitation visualization technique we first seed the fluid with very small bubbles. For this purpose we rotate the top disk rapidly ($\sim$30 Hz) in order to generate a large quantity of bubbles by suction from the free surface. This is easier with a soda water containing dilute carbon dioxide or with soapy water in which surface tension is reduced. When the number of bubbles is large enough, we let the system rest so that the large bubbles move to the surface; only the bubbles of a size of the order of 0.05 mm remain. The two disks are then set in rotation for the turbulence experiment. Because the fluid is strongly stirred, the mean bubble concentration remains stable even during long runs of the experiment.

The introduction of bubbles does not appreciably modify the fluid properties. Our bubbles occupy less than 0.5% of the volume, and although in a bubbly fluid the sound velocity is reduced [15], the Mach number of our flow remains very small. We also believe that the introduction of the bubbles does not affect the turbulence. The bubbles, at all large scales, are advected as a passive scalar. Their only possible activation motion is viscous and within the Kolmogorov dissipation scale [16] ($L_K \approx 10 L_I R_I^{-3/4}$). It is only appreciable in very strong pressure gradients, and, as we will see, does not affect the overall homogeneity of the fluid. Measurements of the power dissipated in the turbulent flow with and without bubbles have also shown it to be strictly identical in the two cases.

The tank is lit with diffuse light from behind so that the bubbles appear dark on a light background. In order to record the three-dimensional structure of the filaments the same region of the fluid is observed in two perpendicular directions with two cameras. We use videotape recorders which provide fifty images of the flow per second. Each image can be taken with a long exposure time (0.01 s); the bubble motion then shows the velocity field. Using a short exposure (0.001 s) we observe more precisely the bubble density.

Once a steady regime of the flow is set, the most evident structures in the flow are the large eddies in the middle region of the cell. They are mostly horizontal and radial, as would be expected from the direction of the main shear. However, our visualization also shows, every now and then, dark filaments with a high concentration of bubbles. Figure 2(a) shows their aspect seen from the side: They form a line a few centimeters long and typically 0.1 mm wide. These scales correspond, respectively, to the energy injection scale L_I and the Kolmogorov dissipation scale L_K. While the large eddies are seen to have lifetimes on the order of 10 times the typical turnover time $\tau_I = \pi L_I/U_I = 2\pi/\Omega_0 \approx 0.1$ s, the filaments of very high concentrations of vorticity only exist during one turnover time. Figure 3(a), a view from the other direction, shows that these structures have a circular section. The photographs seem to show that in these filaments the bubbles often connect to form a hollow tube.

To explain the physical mechanism of our visualization, note that if the experiment is repeated with pure unseeded water these structures are not observed. This means that the local depression is not large enough to spontaneously form vapor cavities. The basic process has to be the migration of the bubbles toward a low-pressure region where they finally gather into a thin hollow tube. This is confirmed by our video recordings with a long exposure time (data not shown), where one can see, surrounding the filament, a cylindrical region of radius $r \approx 2$ mm depleted in bubble concentration. Note that there are enough bubbles in such a volume to form a continuous line along the filament, even with only 0.5% of the volume

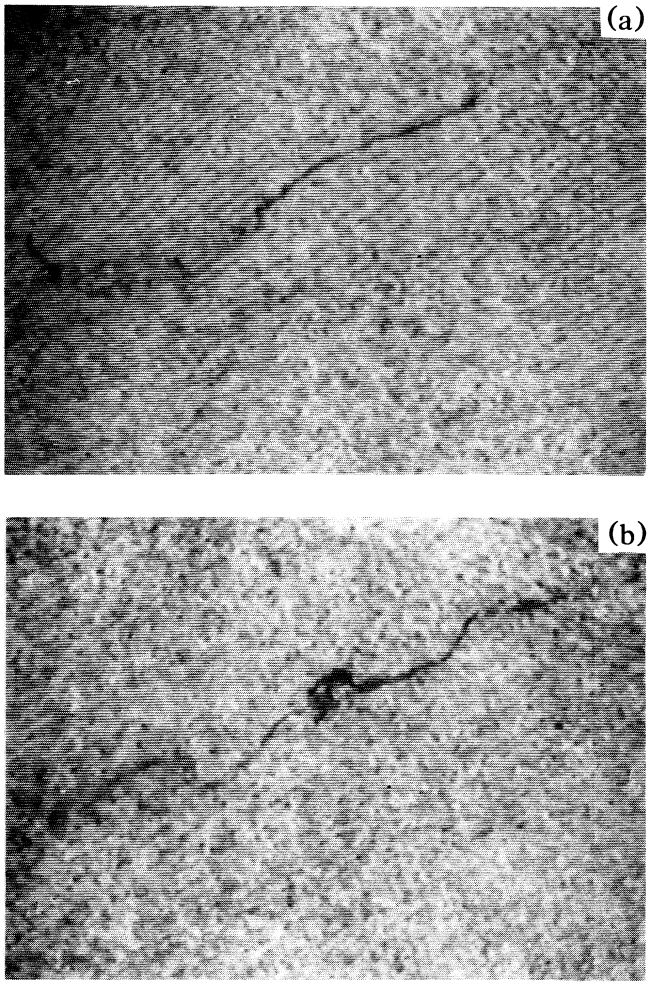

FIG. 2. Detail of two successive video images (taken 0.02 s apart with an exposure time of 0.001 s) showing a side view of a vorticity filament observed in a turbulent flow at a Reynolds number of 80000. Its length is of the order of 5 cm while its diameter (enlarged here by the video image) is of the order of 0.1 mm. (a) The filament at its formation; (b) its destabilization to form kinks.

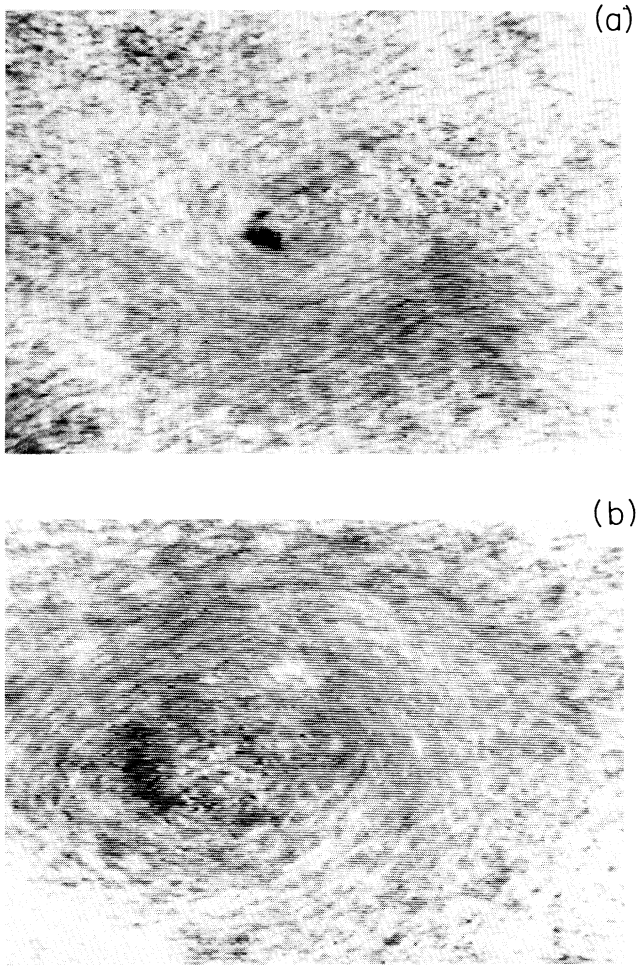

FIG. 3. Two photographs of the evolution of a vorticity filament seen from its extremity. (a) The filament 0.04 s after its formation; (b) 0.1 s later, when it has transformed into a large eddy.

occupied by bubbles.

The high-pressure regions (large σ^2) are also visible as they repel the bubbles, thus having a weaker bubble concentration. These regions are spread out and weakly contrasted. The difference in aspect between the low- and high-pressure regions corresponds to the asymmetry in the pressure histogram obtained in numerical simulation [10]. This histogram has a very long exponential tail only for low pressures corresponding to the vorticity concentration in filaments. Finally, when the fluid is seeded with more bubbles we apparently lower the observation threshold; at a given Reynolds number a greater number of smaller filaments become apparent. This result points to the existence of a hierarchy of filaments with different strengths.

The main characteristic of the filaments is the asymmetry of their evolution, illustrated by the sequence of images shown in Figs. 2(a), 2(b) and 3(a), 3(b). Most of the times, no noticeable structure preexists; structure shows up abruptly in a time of the order of $\frac{1}{50}$ th of a second in the regions of the flow where there is both shear (large ω^2) and convergence (large σ^2) [17]. The filaments usually appear as rather straight lines. Then the formation of helical distortions [18] is observed [visible in Fig. 2(b)]. These distortions appear similar to the kinks which affect the core of long-lived vortices obtained in a rotating tank [19]. In the present experiment these kinks lead to the disintegration of the filaments in a typical time of 0.1 s. After the filaments' disappearance, large, longer-lived eddies remain where they have vanished [Fig. 3(b)] [20].

As there is no physical mechanism available for vortici-

ty generation in the bulk of the flow, vortex line stretching by the strain field must be responsible for vorticity concentration. If there are significant contributions of vorticity itself to the local strain field, they will lead to nonlinear behavior and possibly to a singularity in the inviscid limit [21]. The creation of straight filaments could thus result from some nonlinear "self-focusing" mechanism. The observed asymmetrical time evolution of our filaments might also be evidence of nonlinear behavior. Small viscous effects can also be important by allowing nontrivial changes in vortex line topology through reconnection mechanisms.

In summary, the intermittency observed in time series of the velocity measured at one point has been tentatively ascribed to the advection of relatively stable coherent structures near the point of measurement [3,4]. Observation of the whole turbulent field with our new visualization technique demonstrates the existence and intrinsic intermittency in *both space and time* of regions of high vorticity and their filamentary shape. These filaments appear to have an important role in structuring the flow: They appear in stretched shear regions due to large coherent flows and vanish swiftly, giving birth to large long-lived eddies. We are confident that further experiments using the same technique will help to elucidate the structural properties of turbulence.

We are grateful for useful comments from S. Fauve and E. Siggia. This work was supported by DRET under Contract No. 90/1440.

[1] H. L. Grant, R. W. Stewart, and A. Moilliet, J. Fluid Mech. **12**, 241 (1962).

[2] A. N. Kolmogorov, Dokl. Akad. Nauk. **30**, 301 (1941).

[3] A. Y. S. Kuo and S. Corrsin, J. Fluid Mech. **56**, 447 (1972).

[4] E. Bacry, A. Arneodo, U. Frisch, Y. Gagne, and E. Hopfinger, in *Turbulence and Coherent Structures,* edited by M. Lesieur and O. Métais (Kluwer Academic, Dordrecht, 1990).

[5] E. D. Siggia, J. Fluid Mech. **107**, 375 (1981).

[6] Z. S. She, E. Jackson, and S. A. Orszag, Nature (London) **344**, 6263 (1990); **344**, 226 (1990).

[7] A. Vincent and M. Meneguzzi, J. Fluid Mech. **225**, 1 (1991).

[8] M. E. Brachet, D. I. Meiron, S. A. Orszag, B. G. Nickel, R. H. Morf, and U. Frisch, J. Fluid Mech. **130**, 411 (1983).

[9] M. E. Brachet, C. R. Acad. Sci. Paris **311**, 775 (1990).

[10] M. E. Brachet, in Proceedings of the International Workshop on Novel Experiments and Data Processing for Basic Understanding of Turbulence, Ibaraki, Japan, edited by T. Kambe and K. Kuwahara [Fluid Dyn. (to be published)].

[11] The Taylor-Green vortex [G. I. Taylor and A. E. Green, Proc. Roy. Soc. London A **158**, 499 (1937)] is the three-dimensional flow that develops from the initial conditions $v_x = \sin(x)\cos(y)\cos(z)$, $v_y = -\cos(x)\sin(y)\cos(z)$, $v_z = 0$, following the incompressible Navier-Stokes equations.

[12] K. W. Schwartz, Phys. Rev. Lett. **64**, 415 (1990).

[13] These two secondary toroidal recirculations have maximum strength with plane disks: Because of the boundary layers of the disks the fluid is sucked along the cell's axis and pumped away from the disks along the cell's cylindrical wall. We reduced them by adding protruding rims around these disks (Fig. 1).

[14] In Ref. [8] the fractional energy dissipation per large-eddy turnover time per unit mass was estimated (using a different definition of integral scale velocity $U_I' = U_I/2$) to be 0.7 for the Taylor-Green flow. With this convention our results yield the right order of magnitude: $WL_I M^{-1} U_I'^{-3} \sim 0.7$, where $M = 3$ kg is the total mass of fluid.

[15] D. Y. Hsieh and M. S. Plesset, Phys. Fluids **4**, 970 (1961).

[16] A. S. Monin and A. M. Yaglom, *Statistical Fluid Mechanics* (MIT Press, Cambridge, 1975), Vol. 2.

[17] This organization was observed in Refs. [9] and [10]. Such sudden formation of filaments in regions of convergence is somewhat reminiscent of the formation of dust devils or of tornadoes at the front between cold and hot and humid air.

[18] It is well known that a hollow tube is unstable owing to surface tension. However, this process would generate a peristaltic instability on a small scale, which would be very different from what we observe.

[19] E. J. Hopfinger, F. K. Browand, and Y. Gagne, J. Fluid Mech. **125**, 505 (1982).

[20] We have also seen many events involving the common evolution of several structures. For instance, two filaments of the same direction give rise to two corotating vortices which will coalesce. Before their spooling around each other a weak streamwise secondary filament appears perpendicularly between the two initial structures.

[21] A. Pumir and E. Siggia, Phys. Fluids A **2**, 220 (1990).

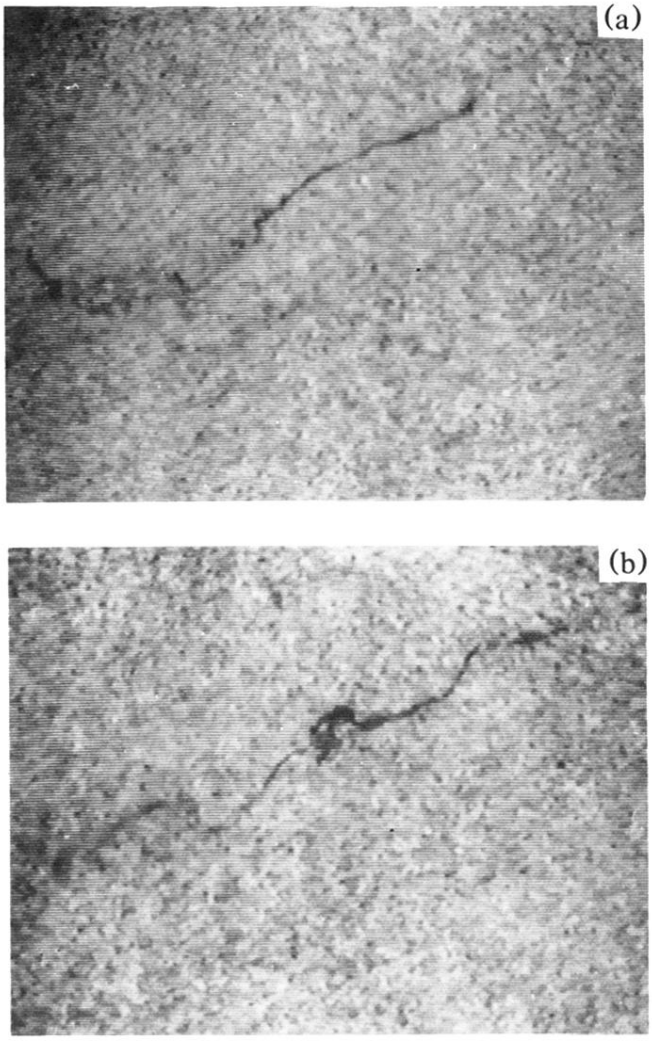

FIG. 2. Detail of two successive video images (taken 0.02 s apart with an exposure time of 0.001 s) showing a side view of a vorticity filament observed in a turbulent flow at a Reynolds number of 80 000. Its length is of the order of 5 cm while its diameter (enlarged here by the video image) is of the order of 0.1 mm. (a) The filament at its formation; (b) its destabilization to form kinks.

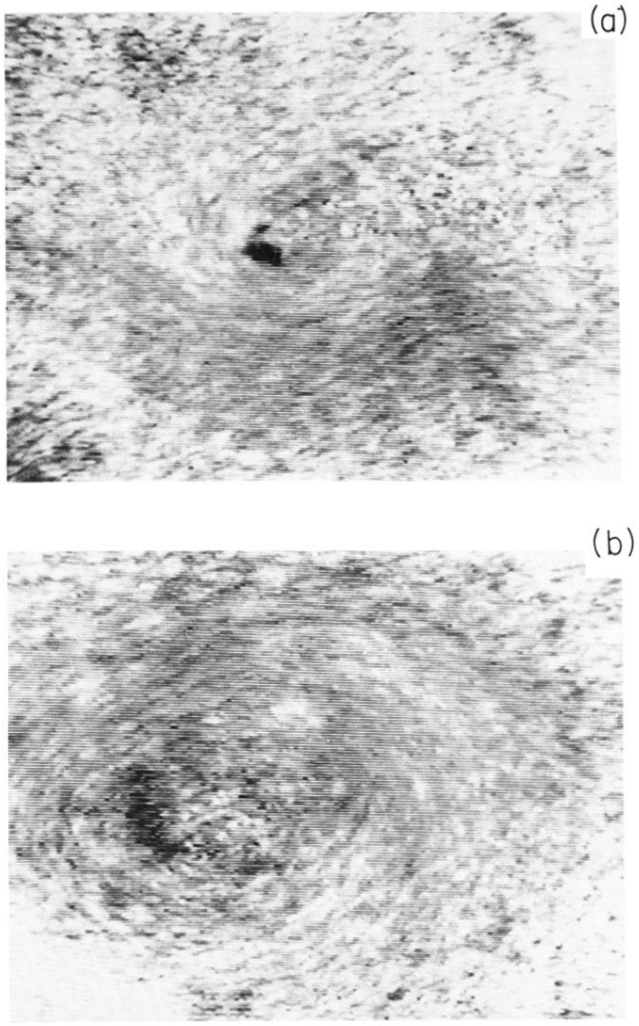

FIG. 3. Two photographs of the evolution of a vorticity filament seen from its extremity. (a) The filament 0.04 s after its formation; (b) 0.1 s later, when it has transformed into a large eddy.